ISSN: 2994-7510

Research Article

Journal of Water Research

Membrane Separation-Based Recovery and Reuse of Textile Wastewater

Pritesh S. Patil[1], Ankita Yadav[2], Nitin V. Thombre[3*], Yagna Prasad K.[4] and Anand V. Patwardhan[1]

[1]*Department of Chemical Engineering, ICT (Mumbai).*

[2]*Department of Fibres and Textile Processing, ICT (Mumbai).*

[3]*VA Tech Wabag, Pune.*

[4]*VA Tech Wabag, Chennai.*

[*]Corresponding Author
Nitin V. Thombre, VA Tech Wabag, Pune.

Submitted: 2024, Nov 01; **Accepted:** 2024, Nov 25; **Published:** 2024, Dec 10

Citation: Patil, P, S., Yadav, A., Thombre, N. V., Prasad, Y. K., Patwardhan, A. V. (2024).Membrane Separation-Based Recovery and Reuse of Textile Wastewater. *J Water Res, 2*(1), 01-10.

Abstract

The textile industry is one of the oldest sectors and consumed different dyes and harmful chemicals for the process. It involves various processes and requires a huge amount of water to carry out these processes, therefore, it is causing a large amount of water pollution. In the present study, we have successfully treated the textile effluent using membrane separation. The effluent was collected from a local effluent treatment plant (ETP) and treated on commercial membranes i.e. polymeric and ceramic, and novel synthesized composite ceramic membrane. Detailed analyses of each membrane were carried out. The effluent procured from the ETP and treated effluent was characterized in terms of pH, total dissolved solids (TDS), chemical oxygen demand (COD), biological oxygen demand (BOD), cconductivity andtturbidity. A reduction in all the measured parameters of water was observed. COD was reduced around 40% after the treatment of effluent. Overall, our novel synthesized composite ceramic membrane shows better results and is comparable to the commercially available membranes.

Keywords: Textile Effluent, Industrial Wastewater Treatment, Membrane Filtration, Ceramic Membranes, Polymeric Membranes

1. Introduction

India's oldest and second-largest employment-creating sector is textile industry. Textile processes are consumed large amount of water in addition to the various dyes and harmful chemicals. The textile industry is utilizing about 60% of total dyes manufactured worldwide [1]. The textile industry is generating large amount of water pollution, which is a major concern with this industry. Typically, the textile industry involves processes such as bleaching, printing, sizing, de-sizing, scouring, finishing, dyeing, and mercerizing [2,3].

The bleaching, finishing, and dyeing processes usually consume near about half of the total water required for the textile industry. Every process results in producing a high amount of effluent [4,5]. various chemicals and auxiliaries used in textile processing include carboxymethyl cellulose, polyvinyl alcohol, sodium hydroxide, sodium carbonate, sodium bicarbonate, hydrogen peroxide, formaldehyde, synthetic dyes, etc. The detailed process-wise major pollutants discharged in the textile processing are enlisted in figure 1 [6].

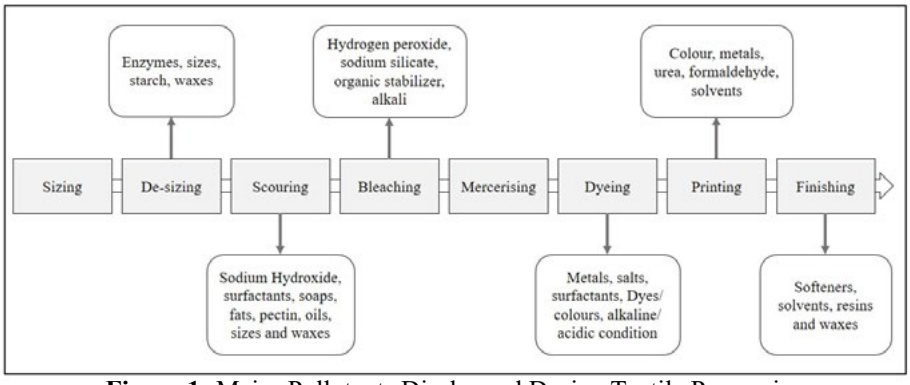

Figure 1: Major Pollutants Discharged During Textile Processing

The auxiliary chemical used for the textile process contains some carcinogenic chemicals such as 2-napthylamine, benzidine, 4-biphenylamine, etc. In addition to these chemicals and auxiliaries, the textile effluent carries various heavy metals such as lead, cobalt, chromium, iron, magnesium, copper, phosphorus, sodium, potassium, etc. in trace amounts [7-10]. The composition of textile effluent is fluctuated in every industry due to changes in process, water utilization, use of different dyes and colours, use of a different type of fibre, different equipment use, etc [11-13]. The location of the industry, the fashion of the society, atmosphere is also included to decide the effluent composition.

Due to notable advantages such as high separation tendency, low energy utilization, stable effluent quality, compact and simple design; membrane separation technology is accepted rapidly throughout. The process is environmentally green as it does not need any chemicals and additives. It is a power ful alternative that can partially tackle the treatment of industrial wastewater. Yadav studied the coke oven wastewater treatment using similar polymeric and ceramic membranes[14]. They have found that the membrane separation technology is efficient and cost-effective alternative to treat industrial effluents.

In the present study, nnanofiltration membranes were employedto treat thetextile effluent from an effluent treatment plant.We have successfully compared performance of our synthesized ceramic membrane with the commercially available ceramic and polymeric membranes.The factors that govern the membrane performanceare membrane flux, membrane permeability, fouling of the membrane (reversible and irreversible), the flux recovery ratio (FRR) and the flux decline ratio (FDR).The effluent was primarily characterized by factors such as BOD, COD, TDS, pH, turbidity, conductivity and osmolality.

2. Materials and Methods

2.1 Materials

The textile effluent was taken from Dombivli common effluent treatment plant (DCETP), Thane. Commercially available hydrophilic polyamide membrane (Microfilt India Private Limited, India) with molecular weight cut-off of 400 Da (400 gm/gmol), as well as commercially available ceramic membrane (Tami Industries, France) with molecular weight cut-off of 1000 Da (1000 gm/gmol) were used.

Then, in-house synthesized ceramic membranes were used to compare the obtained results. All the filtration experiments were carried out in a pressurised and dry nitrogen atmosphere. Deionized water was essential to carry out this study and it was taken from the Sartorius-arium mini plus (Model number: H_2O-MA-UV-T) water purification system. All the chemicals required in the present study were purchased from Alfa Aesar (Germany), Sigma Aldrich (Germany), and Merck (Germany).

2.2 In-House Synthesis and Characterization of Composite Ceramic Membrane

The particle size of ceramic components (alumina and silica) was reduced using a horizontal rotating ball mill with 0.8 mm stainless steel balls. The particle size was reduced to 0-30 µm after 24 hrs of rotation at 40 rpm. The binder solution was prepared at 400 rpm using Polyethylene glycol-200 (PEG-200 (1.78%), PEG-1500 (0.88%), and carboxy-methyl cellulose (CMC) (2.66%) in water. The alumina (89.92%) and silica (4.73%) were then added while stirring the solution vigorously for 12 hrs at 400 rpm.

In result, we get a white slurry which was then put for drying in ambient air for 24 hrs followed by drying in an oven at 60 °C for 12 hrs. The hydraulic press was used to make the ceramic membrane supports using stainless steel die at uniform pressure of 110 Mpa. The cylindrical disc with a thickness of 4 mm and a diameter of 55 mm was heat up at 1700 °C. These discs were then coated by boehmite sol, for this vertical dip coating method was used. These freshly coated membranes were put for drying using ambient air for 24hrs and then calcined at 550 °C to prevent cracking. This coating process continues till we get the anticipated pore size.

The shrinkage and porosity were calculated for the sintered membranes by Archimedes' principle. The pore density was calculated as porosity divided by the area of the pores. The membrane flux was determined. The membrane was analyzed based on Scanning Electron Microscopy (SEM) (FEI quanta-200 Scanning Electron Microscope, Netherlands), Brunauer–Emmet–Teller (BET) analysis, zeta potential (Zetasizer Nano ZS90, Malvern, UK), X-ray diffraction analysis (D8 Advance, Bruker, Germany), Atomic Force Microscopy (AFM) (Veeco diInnova, Bruker, USA), and chemical stability.

2.3 Filtration Setup

For the filtration experiments, both ceramic and polymeric membranes were utilized. The ceramic membrane had an effective surface area of 12.56 cm^2, while the polymeric membrane's surface area was 14.2 cm^2. Figure 2(a) illustrates the filtration setup for the polymeric membrane, and Figure 2(b) depicts the setup for the ceramic membrane. The polymeric membrane experiments were performed using a stirred cell dead-end filtration unit (Sterlitech, model HP4750), whereas the ceramic membrane experiments were conducted with a similar unit from Tami Industries. Pressure was applied using a nitrogen cylinder, and both setups were operated within their respective safe pressure limits.

For the polymeric membrane tests, transmembrane pressures were varied at 5, 10, 15, 20, and 25 bar. In contrast, the ceramic membrane experiments were conducted at pressures of 1, 2, 3, and 4 bar. During all experiments, the feed side was continuously stirred at 500 rpm. To ensure accuracy, each set of experiments was performed in triplicates, and the results are presented as the average of these replicates.

2.4 Compaction of Membrane

The circular membranes were initially immersed in deionized (DI) water to eliminate any particulate matter adhering to their surfaces. Following this cleaning step, membrane compaction was done using deionized water to establish a steady flux using nitrogen

[15]. For the polymeric membranes, compaction was performed by gradually increasing the transmembrane pressure from 5 bar to 25 bar. In the case of the ceramic membranes, the compaction process started at 1 bar and was gradually increased to a maximum of 4 bar.

2.5 Effluent Characteristics

The effluent was analyzed for several key parameters. pH was measured using a pH meter (Eutech, pH Tutor). Turbidity was assessed with a turbidity meter (Equiptronics, Digital Turbidity Meter, model EQ 811). Osmolality was determined using a semi-micro osmometer (Knauer, model K-7400S). TDS (total dissolved solids) and conductivity were measured with portable meters (Thermo Scientific, Orion Star A112 and A122).

Chemical oxygen demand (COD) was analyzed by digesting the effluent sample using a standard for COD (Thermo Scientific, Orion Aquafast, range 0-15000 ppm) in a digester (Thermo Scientific, Orion COD 165 Thermoreactor) at 150°C for 2 hours, followed by COD detection with a sensor (Thermo Scientific, Orion AQ3700). TOC (Total organic carbon) was quantified using a total organic carbon analyzer (Shimadzu Corp., model TOC-L, H564054).

3. Theory and Calculations

3.1 Flux and Permeability of Membranes

The membrane flux and permeability were evaluated by equations (1), and (2), respectively. The flux and permeability experiments were performed using DI water on the membrane before and after the filtration trials.

$$J = {}^{V}/_{A.t} \qquad \text{Eq. (1)}$$

$$P = {}^{J}/_{p} \qquad \text{Eq. (2)}$$

Here, J (expressed in L/m^2.h or LMH) and P (expressed in L/m^2.h.bar or LMH.bar) are the flux and permeability, respectively. The V (expressed in L), t (expressed in s), A (expressed in m^2), and *P* (expressed in bar) are the permeate volume, an interval of a sampling (5 min), filtration surface area for the filtration, and transmembrane pressure, respectively.

3.2 Flux Decline Ratio (FDR) and Flux Recovery Ratio (FRR) of Membranes

$$FDR = \left(\frac{J_0 - J_f}{J_0}\right) x\ 100 \qquad \text{Eq. (3)}$$

$$FRR = \left(\frac{J_{af}}{J_{bf}}\right)\ x\ 100 \qquad \text{Eq. (4)}$$

Here, J_o and J_f (expressed in LMH) denote the initial and final flux, respectively. Whereas, J_{bf} and J_{af} (expressed in LMH) represent the flux before and after filtration, respectively.

The particles get deposited on the membrane surface; as a result, the membrane might be fouled. These antifouling characteristics were analysed by assessing FDR and FRR. The FDR and FRR were calculated by equations 3 and 4.

3.3 Fouling Mechanism

Membrane fouling is a critical challenge in membrane filtration processes, where the performance and longevity of the membranes are compromised by the accumulation of foulants on their surface or within their pores. This phenomenon can lead to increased resistance to flow, reduced permeability, and frequent maintenance or replacement of membranes, resulting in higher operational costs.

Fouling agents can include organic compounds, inorganic salts, microorganisms, and particulate matter, which interact with the membrane material through mechanisms such as adsorption, precipitation, and biofilm formation. Understanding the mechanisms and factors influencing fouling is essential for developing effective strategies to mitigate its impact, such as optimizing operating conditions, employing cleaning techniques, and designing advanced membrane materials with enhanced resistance to fouling [16].

Addressing these issues is crucial for improving the efficiency and sustainability of filtration technologies used in various industries, including water treatment, pharmaceuticals, and food processing. Hermia's model was implemented to prognosticate the fouling mechanism [17]. The permeate flux reduction is defined by the steady transmembrane pressure, upon which the model relies. Table 2 provides an explanation for the model. It was believed that the equation corresponding to the prevailing fouling mechanism would have the highest correlation coefficient (R^2) throughout all experimental conditions.

4. Results and Discussion

4.1 Characterization of in-House Composite Ceramic Membrane

The shrinkage of more than 50% and porosity of more than 30% were estimated at 1700°C calcination temperature. The pore density for the membrane support and coated membrane was observed as 2.59 x 10^{10}m^{-2}, and 4.14 x 10^{13}m^{-2}, respectively. The flux of the membrane after coating was found at 1 bar as 80.19 LMH, which was gradually increased up to 142.47 LMH at 4 bar.

The pore diameter of the membrane support and the coated membrane was investigated in the range of 2-6 µm (almost 5 µm), and 100 nm using the SEM analysis. It is safe to say that the membranes fall under nanofiltration category based on the size of the pores. By using AFM, the membrane surface was observed for membrane roughness, and root mean square roughness and average roughness were found at 89.20 nm and 72.40 nm respectively.

The XRD analysis was conducted to determine phase changes of alumina. For the support, alumina was found in alpha form; whereas, for the boehmite top layer, alumina was found in gamma form. From zeta potential, it was observed that the isoelectric point of the membrane was observed between pH 7-8. The synthesized ceramic membranes were chemically stable in the pH range of 1-12.

4.1.1 Flux of the Membrane

The characteristics of the membranes were evaluated by measuring the deionized (DI) water flux before and after filtration. Initially, the DI water flux was highest, but it decreased following the filtration process. An increase in transmembrane pressure was associated with higher flux rates, likely due to the enhanced driving force overcoming membrane resistance. This pattern was observed across all three membranes i.e. commercial polymeric and ceramic, and freshly synthesized ceramic. Among these, the synthesized ceramic membrane exhibited the highest flux. The variation in water flux for fresh versus used membranes, as well as the effect of transmembrane pressure on flux for each membrane type, is illustrated in Figures 2(a), 2(b), and 2(c).

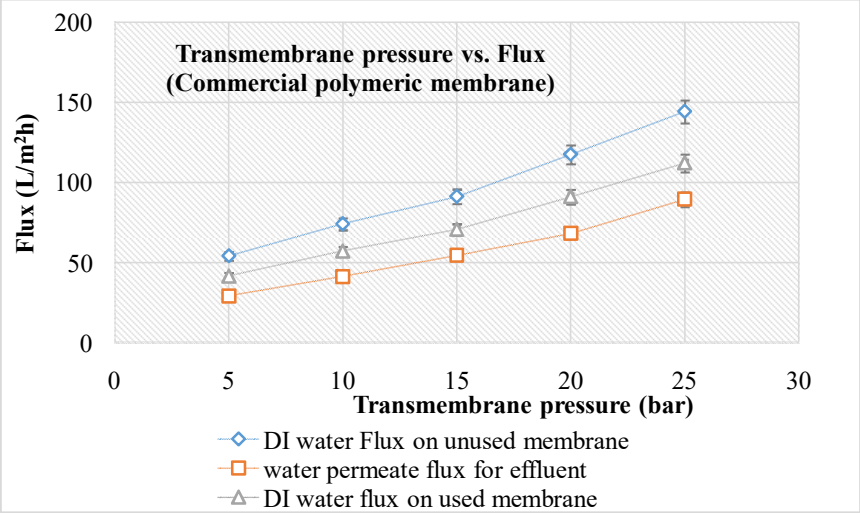

Figure 2: (a) Water Flux for Fresh/Unused Membrane, Used Membrane, and Textile Effluent with a Trans-Membrane Pressure Difference on Commercial Polymeric Membrane.

The initial deionized (DI) water flux for the unused commercial polymeric membrane was measured at 54.28 LMH at 5 bar, which increased progressively to 144.44 LMH at 25 bar. Following filtration, the water flux decreased to 41.75 LMH and 112.23 LMH at 5 bar and 25 bar, respectively. During the filtration process, the flux was lowest at 29.30 LMH at 5 bar and 89.59 LMH at 25 bar.

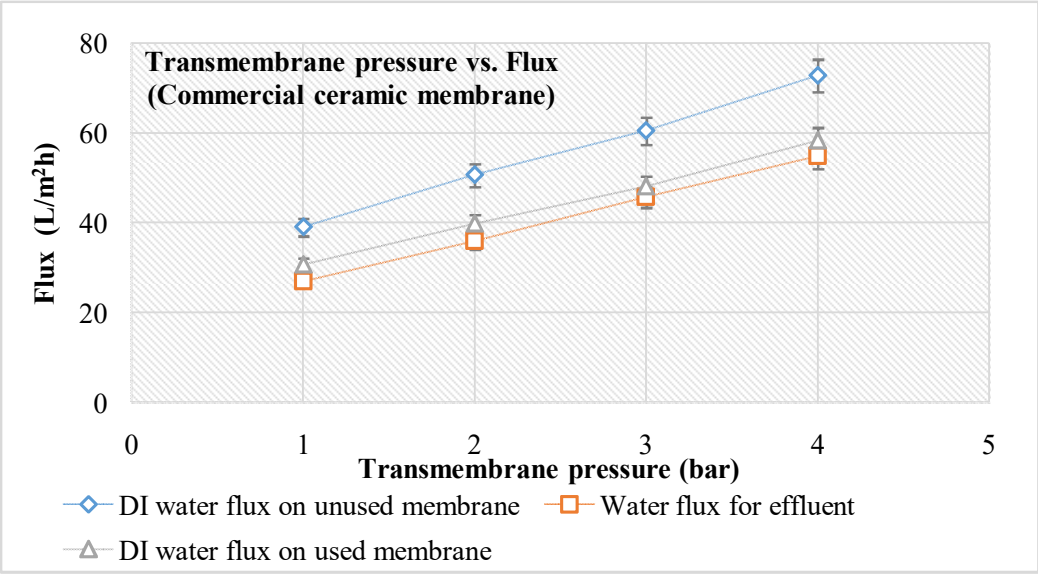

Figure 2: (b) Water Flux for Fresh/Unused Membrane, Used Membrane, and Textile Effluent with a Trans-Membrane Pressure Difference on Commercial Ceramic Membrane.

For the unused commercial ceramic membrane, the initial deionized (DI) water flux was 39.03 LMH at 1 bar, which increased to 72.80 LMH at 4 bar. Post-filtration, due to particle accumulation on the membrane surface, the flux decreased to 30.61 LMH at 1 bar and 58.33 LMH at 4 bar. During filtration, the flux values were 26.91 LMH at 1 bar and 54.82 LMH at 4 bar.

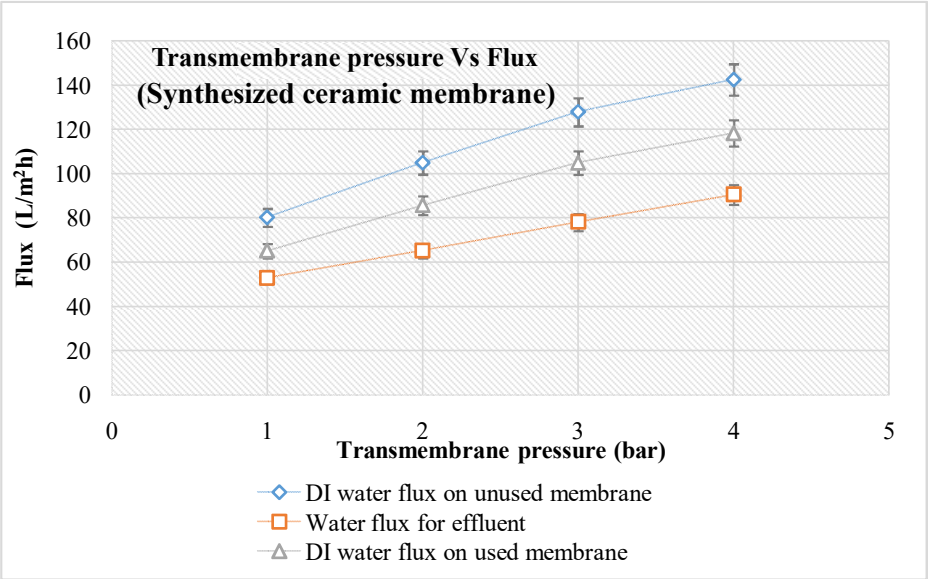

Figure 2: (c) Water Flux for Fresh/Unused Membrane, Used Membrane, and Textile Effluent with a Trans-Membrane Pressure Difference on Synthesized Ceramic Membrane.

For the unused in-house synthesized ceramic membranes, the highest deionized (DI) water flux recorded was 80.19 LMH at 1 bar. Following filtration, this flux decreased to 65.11 LMH at 1 bar. As the transmembrane pressure increased, the flux rose to 142.47 LMH at 4 bar for the unused membranes and 118.30 LMH at 4 bar for the membranes used in filtration. During effluent filtration, the flux values were 52.82 LMH at 1 bar and 90.51 LMH at 4 bar.

4.1.2 Permeability of Membranes

Membranes	Unused membrane	Used membrane
Commercial Polymeric membrane	6.07	4.71
Commercial Ceramic Membrane	20.44	16.26
In-house synthesized ceramic membrane	41.45	34.14

Table 1: Permeability of Fres hand Used Membranes.

Membrane permeability was evaluated using data from permeate flux experiments conducted with deionized (DI) water before and after treatment. The flux data, summarized in Figures 2(a), 2(b), and 2(c), were used to calculate membrane permeability, represented as the slope of the flux versus transmembrane pressure graph (Table 1).

The in-house synthesized ceramic membrane exhibited the highest permeability, while the commercial polymeric membrane had the lowest. Additionally, permeability decreased following effluent filtration, likely due to concentration polarization on the membrane surface. The permeability values for the unused membranes were 6.07 LMH•bar for the commercial polymeric membrane, 20.44 LMH•bar for the commercial ceramic membrane, and 41.45 LMH•bar for the synthesized ceramic membrane. After treatment, these values decreased to 4.71 LMH•bar, 16.26 LMH•bar, and 34.14 LMH•bar, respectively.

4.1.3 FDR and FRR (%)

The FDR (flux decline ratio) and FRR (flux recovery ratio) were analyzed to evaluate the antifouling properties of these membranes. A lower FDR and a higher FRR suggest reduced particle deposition on the membrane surface, indicating less fouling and improved flux performance. It was found that the FDR decreased with increasing transmembrane pressure for all membranes tested. Higher pressure provided a greater driving force for permeate passage, resulting in reduced particle accumulation and consequently lower flux decline.

Similarly, the FRR improved with increasing transmembrane pressure for each membrane type. The enhanced pressure facilitated better permeate flow and minimized particle buildup, leading to higher flux recovery. The variations in FDR and FRR with changes in transmembrane pressure for commercial polymeric, commercial ceramic, and synthesized ceramic membranes are elaborated in Figures 3(a), 3(b), and 3(c), respectively.

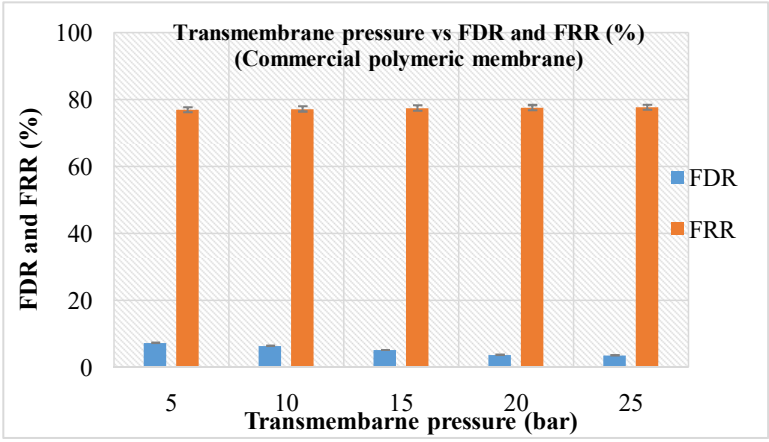

Figure 3: (a) Flux Decline Ratio and Flux Recovery Ratio for Textile Effluent with a Trans-Membrane Pressure Difference on Commercial Polymeric Membrane.

For the commercial polymeric membrane, the FDR was found 7.20 % at 5 bar, which was decreased to 3.51 % at 25 bar. In contrast, FRR slightly increased from 76.91 % at 5 bar to 77.70 % at 25 bar.

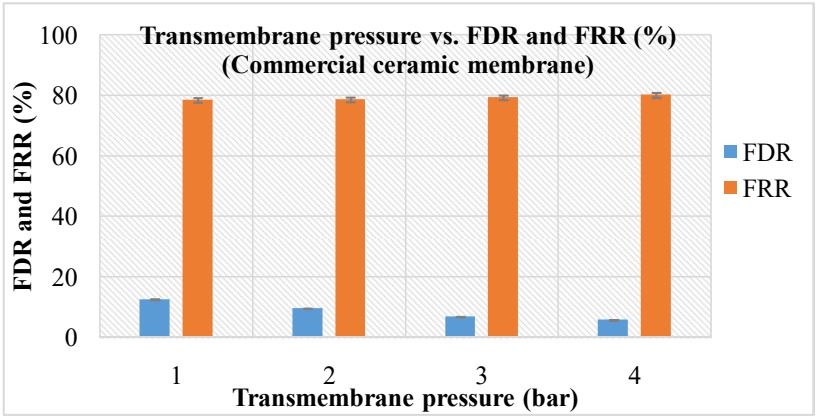

Figure 3: (b) Flux Decline Ratio and Flux Recovery Ratio for Effluent with a Trans-Membrane Pressure Difference on Commercial Ceramic Membrane.

For the commercial ceramic membrane, the FDR (%) was decreased from 12.54 to 5.90 as pressure increased from 1 bar to 4 bar. The FRR (%) was increased from 78.42 at 1 bar to 80.12 at 4 bar.

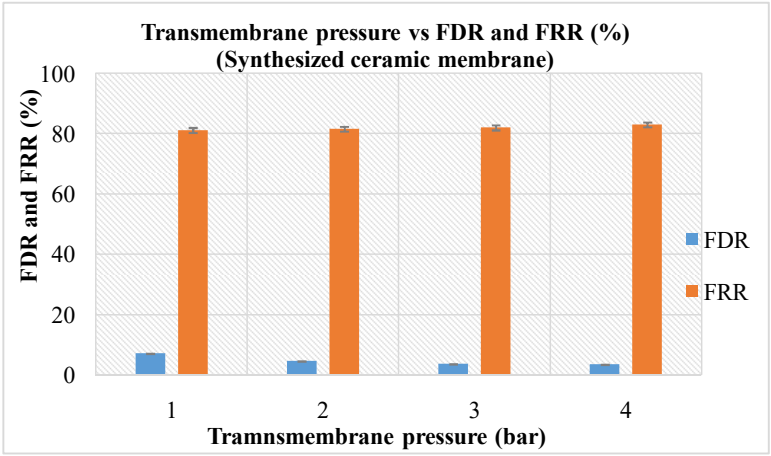

Figure 3: (c) Flux Decline Ratio and Flux Recovery Ratio for Effluent with a Trans-Membrane Pressure Difference on Synthesized Ceramic Membrane.

For synthesized ceramic membrane, the FDR (%) decreased from 7.13 at 1 bar to 3.42 at 4 bar, whereas, FRR (%) increased from 81.20 to 83.03 as transmembrane pressure increased from 1 to 4 bar.

4.2 Fouling Mechanism

The fouling mechanism, which describes the interaction between particles and the membrane surface, was analyzed using Hermia's model. The model that best described the fouling mechanism was identified by the highest correlation coefficient (R^2). The equation yielding the highest R^2 value was considered to represent the predominant fouling mechanism. Experimental R^2 values are detailed in Table 2.

Hermia's fouling mechanism				
Transmembrane Pressure (bar)	**Complete blocking**	**Standard blocking**	**Intermediate blocking**	**Cake layer blocking**
Commercial polymeric membrane				
5	0.9886	0.9897	0.9908	0.9928
10	0.9842	0.9853	0.9863	0.9883
15	0.9766	0.9777	0.9788	0.9808
20	0.9963	0.9964	0.9966	0.9969
25	0.9740	0.9748	0.9756	0.9772
Commercial ceramic membrane				
1	0.9872	0.9892	0.9911	0.9943
2	0.9930	0.9941	0.9952	0.9969
3	0.9930	0.9939	0.9946	0.9960
4	0.9909	0.9917	0.9925	0.9939
In-house ceramic membrane				
1	0.9944	0.9951	0.9958	0.9970
2	0.9948	0.9953	0.9958	0.9966
3	0.9866	0.9872	0.9878	0.9889
4	0.9804	0.9810	0.9817	0.9829

Table 2: Regression Coefficient (R^2) in Fouling of the Membrane.

R^2 values from all experiments indicated that the cake-layer blocking mechanism consistently had the highest correlation. This model indicates the pore blocking by cake-layer was the governing fouling mechanism across all tested transmembrane pressures during textile effluent filtration. Consequently, the cake-layer blocking model emerged as the most accurate representation of membrane fouling in this study.

4.3 Scanning Electron Microscopy (SEM)

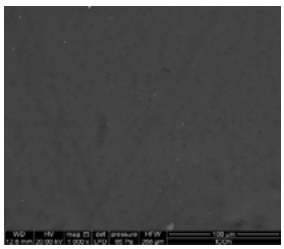

(a) Unused commercial polymeric membrane

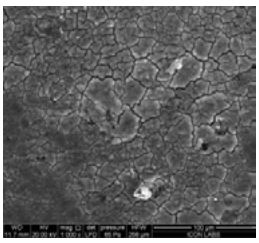

(b) Used commercial polymeric membrane

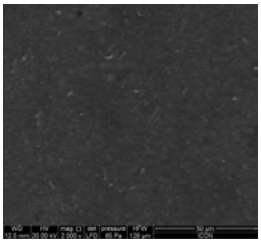

(c) Unused commercial ceramic membrane

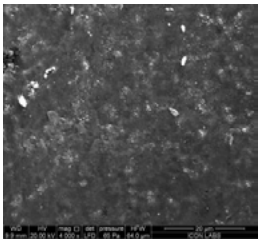

(d) Used commercial ceramic membrane

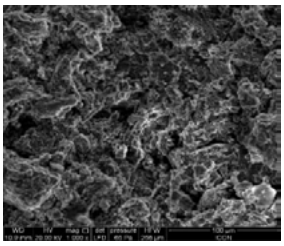

(e) Unused synthesized ceramic membrane

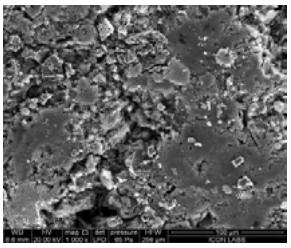

(f) Used synthesized ceramic membrane

Figure 4: Scanning Electron Microscopy Images of Fresh/Unused and Used Membranes.

The surface morphology of both, fresh and used membranes—commercial polymeric and ceramic and synthesized ceramic—was examined using Scanning Electron Microscopy (SEM). Figures 4(a), 4(c), and 4(e) display the surface images of the unused commercial polymeric, commercial ceramic, and synthesized ceramic membranes, respectively. In contrast, Figures 4(b), 4(d), and 4(f) show the deposition of effluent particles on the surfaces of the used commercial polymeric, commercial ceramic, and synthesized ceramic membranes. The SEM images reveal an uneven distribution of particles, which supports the Hermia's model of fouling. This model accurately reflects the observed particle deposition, resembling a cake layer on the membrane surfaces.

4.4 Atomic Force Microscopy (AFM)

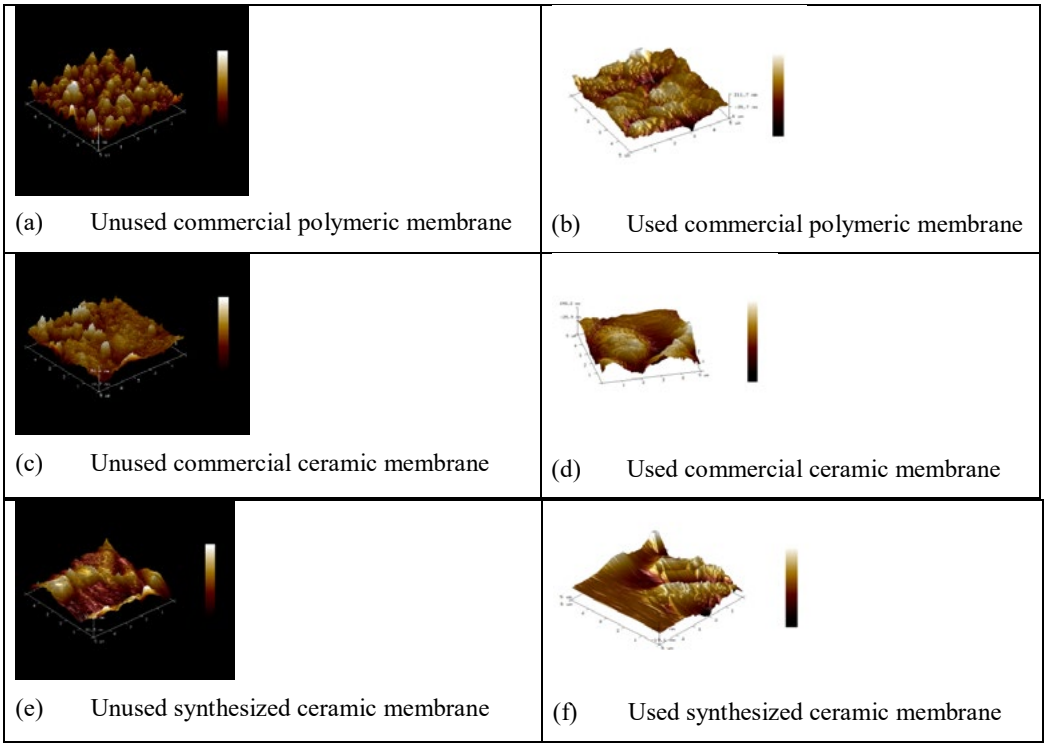

(a) Unused commercial polymeric membrane

(b) Used commercial polymeric membrane

(c) Unused commercial ceramic membrane

(d) Used commercial ceramic membrane

(e) Unused synthesized ceramic membrane

(f) Used synthesized ceramic membrane

Figure 5: Atomic Force Microscopy Images of Unused and Used Membranes.

Membrane		**RMS roughness (Rq) (nm)**	**Average roughness (Ra) (nm)**
Commercial polymeric	Unused	33.90	27.20
	Used	64.5	47.6
Commercial ceramic	Unused	13.40	9.77
	Used	90	68.3
Synthesized ceramic	Unused	89.20	72.40
	Used	86.8	59.9

Table 3: Surface Roughness Data of Unused and Used Membranes

Figures 5(a), 5(c), and 5(e) display the Atomic Force Microscopy (AFM) images of the unused commercial polymeric, commercial ceramic, and synthesized ceramic membranes. Figures 5(b), 5(d), and 5(f) show the surface of these membranes after exposure to effluent, revealing particle deposition. The RMS roughness (root mean square) and average roughness were observed and summarized in Table 3 for all the membranes. The highest roughness was observed in the unused synthesized ceramic membranes, which slightly decreased in the used membranes due to cake layer deposition, as indicated by SEM images. Conversely, for the commercially available membranes (both polymeric and ceramic), a gradual increase in surface roughness was noted, likely due to the extensive and uneven particle accumulation on the membrane surfaces.

4.5 Effluent Characterization and COD Reduction

The ligands/information title should be placed under the images. First image for commercial polymeric, second image for commercial ceramic and third for synthesized ceramic membrane.

Figure 6: Images of Textile Effluent and Treated Effluent Samples.

Figure 6 presents images of both the effluent and the treated effluent samples. These samples were analyzed for various parameters, with detailed results summarized in Table 4.

Textile effluent contains high concentrations of pollutants, including elevated levels of total dissolved solids (TDS), chemical oxygen demand (COD) and osmolality. Especially high COD and osmolality values present in the effluent cause difficulty in recovery of the water and its reuse in the textile industry again. Nanofiltration membranes are used in this study as a pre-treatment tend to reduce the COD and osmolality load on the reverse osmosis membranes downstream in the effluenyt treatment plant (ETP).A comparative analysis of filtration through ceramic and polymeric membranes revealed similar outcomes for both types.

Post-treatment, all measured parameters—conductivity, turbidity, osmolality, COD, and TOC—showed an anticipated decrease. The filtration process effectively removed some particles, leading to a significant reduction in TOC, total dissolved solids (TDS), and turbidity in the treated samples. Notably, there was a substantial decrease in both COD and TOC as a result of the Nanofiltration treatment. Similar results were obtained by Many researchers in the past have studied different technologies to reduce COD and color from textile wastewater and they found similar results in their study [18-20].

Parameters			**pH**	**TDS (ppm)**	**Cond. (mhos/cm)**	**Turbidity (NTU)**	**Osmolality (mOsmol)**	**TOC (ppm)**	**COD (ppm)**
Effluent		Bar	8.4	1572	3.21	23.8	51	514	1600
Treated effluent	**On commercial polymeric membrane**	5	8.39	1486	3.05	17.2	44	408	960
		10	8.37	1484	3.02	16.9	43	408	960
		15	8.39	1477	3.01	17.1	44	408	960
		20	8.42	1473	3.00	17.1	42	404	960
		25	8.38	1482	2.97	16.9	40	408	960
	On Commercial ceramic membrane	1	8.32	1491	3.14	20.7	44	395	1280
		2	8.30	1485	3.14	20.4	46	397	1280
		3	8.34	1490	3.12	20.5	45	395	1280
		4	8.31	1492	3.13	20.5	47	396	1280
	On synthesized ceramic membrane	1	8.28	1478	3.08	18.2	46	392	1280
		2	8.25	1475	3.07	18.4	44	390	1280
		3	8.26	1479	3.08	18.4	42	392	1280
		4	8.28	1477	3.06	18.5	43	392	1280

Table 4: Characterization of Untreated and Treated Effluents

5. Conclusion

This study explored the effectiveness of membrane nanofiltration for treating textile industry effluent. The investigation utilized commercial polymeric, commercial ceramic, and synthesized ceramic membranes in a dead-end filtration setup. Comprehensive experimental data were gathered, including measurements of flux for permeate, permeability of membrane, FDR, FRR, and membrane fouling. Additionally, the membranes were analysed using scanning electron microscopy (SEM) and atomic force microscopy (AFM). The treated effluent was evaluated for pH, total dissolved solids (TDS), total organic carbon (TOC), conductivity, turbidity, osmolality, and chemical oxygen demand (COD). Notably, nanofiltration significantly reduced COD levels in the effluent. The results underscore the potential of nanofiltration for treating dye industry effluent and provide valuable data for scaling up the process to an industrial level.

Acknowledgement

We acknowledge the support of time and facilities from Institute of Chemical Technology, Mumbai and VA Tech Wabag Ltd for this study.

Declaration of Competing Interest

The authors declare that they have no known competing financial interests or personal relationships that could have appeared to influence the work reported in this paper

Credit Authorship Contribution Statement

Pritesh S. Patil: conceptualization, carried out experiments,manuscript writing.

Ankita Yadav: formal analysis, editing, regular discussion.

Nitin V. Thombre: resources, writing and review of manuscript, supervision

Yagna Prasad K.: resources, supervision, review.

Anand V. Patwardhan: conceptualization, supervision, review.

References

1. Arvin, E. (1983). Observations supporting phosphate removal by biologically mediated chemical precipitation–A review. *Water Science and Technology, 15*(3-4), 43-63.
2. Babu, B. R., Parande, A. K., Raghu, S., & Kumar, T. P. (2007). Cotton textile processing: Waste generation and effluent treatment.
3. Rongrong, L., Xujie, L., Qing, T., Bo, Y., & Jihua, C. (2011). The performance evaluation of hybrid anaerobic baffled reactor for treatment of PVA-containing desizing wastewater. *Desalination, 271*(1-3), 287-294.
4. Radha, K. V., Sridevi, V., & Kalaivani, K. (2009). Electrochemical oxidation for the treatment of textile industry wastewater. *Bioresource Technology, 100*(2), 987-990.
5. Carmen, Z., & Daniela, S. (2012). *Textile organic dyes-characteristics, polluting effects and separation/elimination procedures from industrial effluents-a critical overview* (Vol. 3, pp. 55-86). Rijeka: IntechOpen.
6. Holkar, C. R., Jadhav, A. J., Pinjari, D. V., Mahamuni, N. M., & Pandit, A. B. (2016). A critical review on textile wastewater treatments: possible approaches. *Journal of environmental management, 182*, 351-366. .
7. Bhuvaneswari, A., Asha, B., & Selvakumar, D. (2016). Isolation and biochemical identification in an anaerobic baffled reactor for the treatment of textile wastewater. I*nternational Journal of ChemTech Research, 9*(3), 645-652.
8. Manekar, P., Patkar, G., Aswale, P., Mahure, M., & Nandy, T. (2014). Detoxifying of high strength textile effluent through chemical and bio-oxidation processes. *Bioresource technology, 157*, 44-51.
9. Imtiazuddin, S. M., Mumtaz, M., & Mallick, K. A. (2012). Pollutants of wastewater characteristics in textile industries. *Journal of Basic & Applied Sciences, 8*(2), 554-556.
10. Hussain, T., & Wahab, A. (2018). A critical review of the current water conservation practices in textile wet processing. *Journal of Cleaner Production, 198*, 806-819.
11. Patil, P. S., Thombre, N. V., K, Y. P., & Patwardhan, A. V. (2023). Studies in nanofiltration of dyes industry effluent. *Indian Chemical Engineer, 65*(2), 155-167.
12. Joshi, V. J., & Santani, D. D. (2012). Physicochemical characterization and heavy metal concentration in effluent of textile industry. *Universal Journal of environmental research & technology, 2*(2).
13. Elango, G., Rathika, G. and Elango, S., 2017. Physico-Chemical Parameters of Textile Dyeing Effluent and Its Impacts with Case study. International Journal of Research in Chemical and Environmental Sciences, 7(1), pp.17–24.
14. Yadav, A. A., Salekar, S. D., Thombre, N. V., Saxena, G. S., & Patwardhan, A. V. (2024). Coke oven wastewater treatment using polymeric and ceramic membranes. *Environmental Science and Pollution Research*, 1-14.
15. Agboola, O., Maree, J., & Mbaya, R. (2014). Characterization and performance of nanofiltration membranes. *Environmental chemistry letters, 12*, 241-255.
16. Thombre, N. V., Gadhekar, A. P., Patwardhan, A. V., & Gogate, P. R. (2020). Ultrasound induced cleaning of polymeric nanofiltration membranes. *Ultrasonics sonochemistry, 62*, 104891.
17. Pereira, G. L. D., Cardozo-Filho, L., Jegatheesan, V., & Guirardello, R. (2023). Generalization and expansion of the Hermia model for a better understanding of membrane fouling. *Membranes, 13*(3), 290.
18. Hanumanthappa, S., Guruswamy, A. D., Eshanna, M. S., & Gaonkar, G. V. (2022). Removal of cod from real textile wastewater using three low-cost adsorbents-its kinetic models and adsorption isotherms. *International Journal of Environmental Analytical Chemistry*, 1-15.
19. Chakraborty, S., Purkait, M. K., DasGupta, S., De, S., & Basu, J. K. (2003). Nanofiltration of textile plant effluent for color removal and reduction in COD. *Separation and purification Technology, 31*(2), 141-151.
20. Aouni, A., Fersi, C., Ali, M. B. S., & Dhahbi, M. (2009). Treatment of textile wastewater by a hybrid electrocoagulation/nanofiltration process. *Journal of hazardous materials, 168*(2-3), 868-874.